Separation Science and Technology
Publication details, including instructions for authors and subscription information:
http://www.informaworld.com/smpp/title~content=t713708471

Improvement in Performance of Thermal Diffusion Columns on Heavy Water Enrichment under Sidestream Operations and Flow-Rate Fraction Variations

Chii-Dong Ho[a]; Sheng-Hung Chen[a]
[a] Department of Chemical and Materials Engineering, Tamkang University, Taipei, Taiwan, R.O.C.

Online publication date: 08 July 2010

To cite this Article Ho, Chii-Dong and Chen, Sheng-Hung(2004) 'Improvement in Performance of Thermal Diffusion Columns on Heavy Water Enrichment under Sidestream Operations and Flow-Rate Fraction Variations', Separation Science and Technology, 39: 14, 3373 — 3403

To link to this Article: DOI: 10.1081/SS-200028904
URL: http://dx.doi.org/10.1081/SS-200028904

SEPARATION SCIENCE AND TECHNOLOGY
Vol. 39, No. 14, pp. 3373–3403, 2004

Improvement in Performance of Thermal Diffusion Columns on Heavy Water Enrichment under Sidestream Operations and Flow-Rate Fraction Variations

Chii-Dong Ho* and Sheng-Hung Chen

Department of Chemical and Materials Engineering, Tamkang University, Tamsui, Taipei, Taiwan, R.O.C.

ABSTRACT

Development of the separation equation in a classical Clusius-Dickel column with sidestream operations for the heavy water enrichment has been accomplished theoretically. Performance of the modified Clusius-Dickel column with sidestream operations and its corresponding maximum separation was determined with the sidestream flow-rate ratio at the feed position and top flow-rate fraction as parameters. The effect of the sidestream operation of a modified Clusius-Dickel column on separation efficiencies for the H_2O-HDO-D_2O system has been

*Correspondence: Chii-Dong Ho, Department of Chemical and Materials Engineering, Tamkang University, Tamsui, Taipei, Taiwan 251, R.O.C.; Fax: 886-2-26209887; E-mail: cdho@mail.tku.edu.tw.

DOI: 10.1081/SS-200028904 0149-6395 (Print); 1520-5754 (Online)

investigated theoretically and experimentally. The theoretical predictions were in good agreement with the experimental results. The theoretical results indicated that the maximum separation efficiency increases with the side stream flow-rate fraction but decreases with feed flow rate and are represented graphically and compared with that in a classical Clusius-Dickel column. Considerable improvement in the device performance is obtained by employing a modified Clusius-Dickel column under sidestream operations and flow-rate fraction variations, instead of using a classical Clusius-Dickel column.

Key Words: Thermal diffusion; Sidestream operations; Separation efficiency; Heavy water enrichment.

INTRODUCTION

Thermal diffusion is an unconventional technique for separating isotopes and rare gases. The separation technique is relatively expensive for energy consuming due to the large temperature difference between the hot and cold walls, so the possible application is limited to highly valuable substances for the economic sense. It was first used to separate uranium at Oak Ridge during World War II[1,2] and several theoretical and experimental approaches have been presented[3–5] for the enrichment of heavy water in the Clusius-Dickel column recently. Clusius and Dickel[6,7] first proposed the separation mechanism and later Furry et al.[8,9] developed a complete theory presentation of producing a cascading effect for a Clusius-Dickel column.

Thermal diffusion combines the well-known fact that a net mass transport in the radial direction resulted from a temperature gradient and density differences resulting in convective flow near the hot and cold walls. For the heavy water enrichment by thermal diffusion in the H_2O-HDO-D_2O system coupled with the equilibrium relation $H_2O + D_2O \Leftrightarrow 2HDO$, the desired material D_2O, which moves toward the cold region, is carried downward by the convective flow in the environs of the cold wall and concentrated in the bottom basin. In fact, the significant factor of convective flow creates the desirable cascading effect and undesirable remixing effect. Many attempts have been made to change convective flow pattern either by suppressing the remixing effect or enhancing the cascading effect, leading to improved thermal diffusion columns with inclination,[10] rotation,[11] moving wall,[12] packing,[13] and winding a wire helix.[14]

The scrubber strategy is to remove most of the airborne dust from the blowing system or SO_2/NO_x from the flue gas. It is natural to speculate on the applicability of a scrubber to air pollution problems,[15,16] blowing ventilation,[17,18] and gas cleaning.[19,20] The sidestream operation may act as the same role as a scrubber in the removal process and thus the separation efficiency improvement in thermal diffusion columns is expected. In the present study, a different approach is proposed to improve the separation efficiency in thermal diffusion columns under sidestream operations at the feed position with flow-rate fraction variations. The separation efficiency enhancement in thermal diffusion columns with sidestream operations was compared with that in a classical Clusius-Dickel column without sidestream operations under the same working dimensions. There are two purposes in the present work: first, to develop the theoretical formulation for thermal diffusion columns with sidestream operations; second, to investigate the effects of the sidestream operation on separation efficiency and the separation efficiency improvement, with the sidestream flow-rate fraction at the feed position and the sidestream and top stream flow-rate fractions as parameters.

MATHEMATICAL FORMULATIONS

Equal Mass Flow Rates at Top and Bottom Ends with Sidestream Operations

Consider a continuous concentric-tube thermo-gravitational thermal diffusion column of the thickness $2w$ between hot and cold plates filled with water isotopes, as shown in Fig. 1 with $r = \sigma_P/\sigma_T = \sigma_P/\sigma$ under the equal mass flow rate of both top and bottom product streams ($\sigma_T = \sigma_B = \sigma$). The classical Clusius-Dickel column is the feed introduced at the center of the column without the sidestream operations. The transport equation of heavy water enrichment under sidestream operations with top and bottom product streams withdrawn of equal mass flow rates at both ends, and the feed introduced at the position L_s from the top of the column and sidestream withdrawn at the opposite side of the feed position, may be modified from the classical Clusius-Dickel column[21] as follows:

$$\tau_e = -\sigma C_B = -\sigma C_e + HC_e\hat{C}_e - K\frac{dC_e}{dz} \tag{1}$$

for the enriching section and

$$\tau_s = \sigma C_T = \sigma C_s + HC_s\hat{C}_s - K\frac{dC_s}{dz} \tag{2}$$

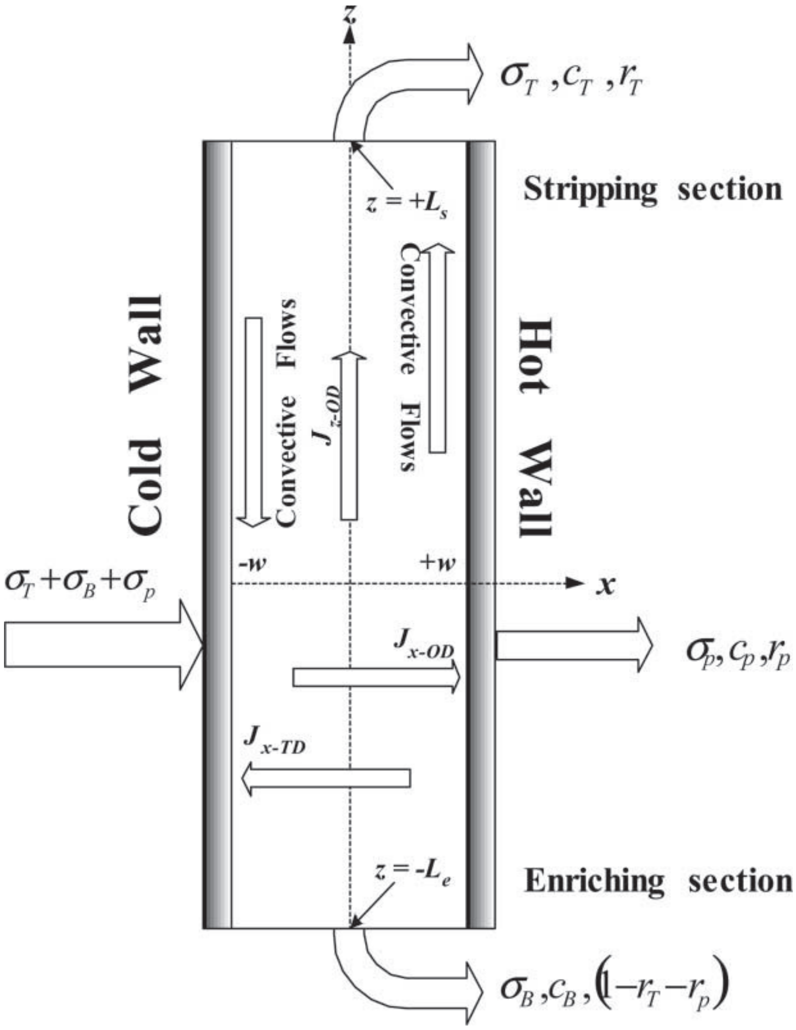

Figure 1. Schematic diagram of a continuous thermal-diffusion column with sidestream withdrawn at the feed position under flow-rate fraction variations.

for the stripping section. The transport constants in the above equations are defined by

$$H = \frac{\alpha\overline{\beta_T}\bar{\rho}g(2w)^3B(\Delta T)^2}{6!\mu\overline{T}} < 0 \quad \text{for } \alpha < 0 \tag{3}$$

and

$$K = \frac{\bar{\rho} g^2 \overline{\beta_T}^2 (2w)^7 B (\Delta T)^2}{9! \mu^2 D} + 2w\bar{\rho}DB \tag{4}$$

while the pseudo concentration products, $C_e\hat{C}_e$ and $C_s\hat{C}_s$ defined in Eq. (5) for enriching and stripping sections, respectively, were defined as

$$C\hat{C} = C\left\{0.05263 - (0.05263 - 0.0135K_{eq}) \times C - 0.027\left\{\left[1 - \left(1 - \frac{K_{eq}}{4}\right)C\right]CK_{eq}\right\}^{1/2}\right\} \tag{5}$$

in which the equilibrium constant K_{eq} for the following equilibrium relation

$$H_2O + D_2O \Longleftrightarrow 2HDO \tag{6}$$

is

$$K_{eq} = \frac{C_2^2}{C_1 C_3} = \frac{[HDO]^2}{[H_2O][D_2O]} \times \frac{19 \times 19}{18 \times 20} \tag{7}$$

The values of the equilibrium constant are $K_{eq} = 3.80$ and 3.793, respectively, at $T = 25°C$ and 30.5°C.[22] There are only slight differences within the operating temperature range.

The pseudo concentration products in Eqs. (1) and (2) are linearized for rather reasonable approximations $C_s\hat{C}_s = a_s + b_sC_s$ and $C_e\hat{C}_e = a_e + b_eC_e$, and Eqs. (1) and (2) reduce to

$$\frac{dC_s}{dz'} = \sigma'(C_s - C_T) + C_s\hat{C}_s = \sigma'(C_s - C_T) + a_s + b_sC_s \tag{8}$$

$$\frac{dC_e}{dz'} = \sigma'(C_B - C_e) + C_e\hat{C}_e = \sigma'(C_B - C_e) + a_e + b_eC_e \tag{9}$$

with the boundary conditions

$$C_e = C_s = C_P \quad \text{at} \quad z' = 0 \tag{10}$$

$$C_s = C_T \quad \text{at} \quad z' = L'_s \tag{11}$$

$$C_e = C_B \quad \text{at} \quad z' = -L'_e \tag{12}$$

and the following dimensionless variables

$$z' = \frac{Hz}{K}, \ \sigma' = \frac{\sigma}{H}, \ \zeta = \frac{L_s}{L} = \frac{L'_s}{L'}, \ L'_s = L'\zeta, \ L'_e = L'(1 - \zeta) \tag{13}$$

The degrees of separation, Δ_e and Δ_s, in the enriching and stripping sections, respectively, were obtained by integrating Eqs. (8) and (9) with the use of Eqs. (10)–(12). The results are

$$\Delta_s = C_P - C_T = \frac{a_s + b_s C_P}{b_s e^{-L'\zeta(b_s+\sigma')} + \sigma'}\left[e^{-L'\zeta(b_s+\sigma')} - 1\right] \tag{14}$$

$$\Delta_e = C_B - C_P = \frac{a_e + b_e C_P}{-b_e e^{L'(1-\zeta)(b_e-\sigma')} + \sigma'}\left[e^{L'(1-\zeta)(b_e-\sigma')} - 1\right] \tag{15}$$

Combination of Eqs. (14) and (15) yields the degree of the separation for the whole column as

$$\Delta = C_B - C_T = \Delta_e + \Delta_s \tag{16}$$

The appropriate values of a_e, b_e, a_s, and b_s may be determined separately from C_P to C_B in the enriching section and from C_T to C_P in the stripping section by the least-square method. Accordingly, minimizing the following integration

$$\min R_s = \int_{C_T}^{C_P} \left[(a_s + b_s C_s) - C_s \hat{C}_s\right]^2 dC_s \tag{17}$$

and

$$\min R_e = \int_{C_P}^{C_B} \left[(a_e + b_e C_e) - C_e \hat{C}_e\right]^2 dC_e \tag{18}$$

Consequently one obtains

$$a_s = \frac{-b_s}{2}(C_T + C_P) + a_{s,0}, \quad a_{s,0} = \frac{1}{\Delta_s}\int_{C_T}^{C_P} C_s \hat{C}_s \, dC_s \tag{19}$$

$$b_s = 12 b_{s,0} - \frac{6 a_{s,0}(C_T + C_P)}{\Delta_s^2}, \quad b_{s,0} = \frac{1}{\Delta_s^3}\int_{C_T}^{C_P} C_s^2 \hat{C}_s \, dC_s \tag{20}$$

$$a_e = \frac{-b_e}{2}(C_B + C_P) + a_{e,0}, \quad a_{e,0} = \frac{1}{\Delta_e}\int_{C_P}^{C_B} C_e \hat{C}_e \, dC_e \tag{21}$$

$$b_e = 12 b_{e,0} - \frac{6 a_{e,0}(C_B + C_P)}{\Delta_e^2}, \quad b_{e,0} = \frac{1}{\Delta_e^3}\int_{C_P}^{C_B} C_e^2 \hat{C}_e \, dC_e \tag{22}$$

Making material balance around the entire column yields the concentration at the feed position

$$\sigma_F C_F = \left(2\sigma + \sigma_p\right) C_F = \sigma C_T + \sigma C_B + \sigma_P C_P \tag{23}$$

or

$$C_P = C_F - \frac{\Delta_e - \Delta_s}{2 + r} \tag{24}$$

where $r = \sigma_P/\sigma$ is the mass flow-rate ratio of the sidestream product to that of the top or bottom product stream. For the column without sidestream operations, that is, $r = 0$, Eqs. (14) and (15) could be reduced to the equations of the classical Clusius-Dickel column. Substitution of Eqs. (19)–(22) and (24) into Eqs. (14) and (15) gives Δ_s and Δ_e in the implicit form and the values of Δ_s and Δ_e may be determined by the successive iteration method.

The concentrations of top and bottom product streams are thus calculated from Eqs. (14), (15), and (24)

$$C_T = C_P - \Delta_s = C_F - \frac{\Delta_e + (1 + r)\Delta_s}{2 + r} \tag{25}$$

$$C_B = C_P + \Delta_e = C_F + \frac{(1 + r)\Delta_e + \Delta_s}{2 + r} \tag{26}$$

Mass Flow-Rate Fraction Variations at Top End with Sidestream Operations

Following the same derivation procedure in the previous section, the transport equation of heavy water enrichment for continuous operations with mass flow-rate fraction variations of top product stream under sidestream operations, as shown in Fig. 1, was obtained accordingly

$$\frac{dC_s}{dz'} = \sigma'_T (C_s - C_T) + C_s \hat{C}_s = \sigma'_T (C_s - C_T) + a_s + b_s C_s \tag{27}$$

$$\frac{dC_e}{dz'} = \sigma'_B (C_B - C_e) + C_e \hat{C}_e = \sigma'_B (C_B - C_e) + a_e + b_e C_e \tag{28}$$

in which $\sigma'_T = \sigma_T/H$ and $\sigma'_B = \sigma_B/H$.

The results of the degrees of separation, Δ_e and Δ_s, in the enriching and stripping sections, respectively, were readily obtained by

$$\Delta_s = C_P - C_T = \frac{a_s + b_s C_P}{b_s e^{-L'\zeta(b_s+\sigma'_T)} + \sigma'_T}\left[e^{-L'\zeta(b_s+\sigma'_T)} - 1\right] \tag{29}$$

$$\Delta_e = C_B - C_P = \frac{a_e + b_e C_P}{-b_e e^{L'(1-\zeta)(b_e-\sigma'_B)} + \sigma'_B}\left[e^{L'(1-\zeta)(b_e-\sigma'_B)} - 1\right] \tag{30}$$

and the values of a_e, b_e, a_s, and b_s are thus calculated using Eqs. (17) and (18) except that the concentration at the feed position was determined by the material balance around the entire column with different mass-flow rates at both top and bottom product streams

$$\sigma_F C_F = (\sigma_T + \sigma_B + \sigma_P)C_F = \sigma_T C_T + \sigma_B C_B + \sigma_P C_P \tag{31}$$

or

$$C_P = C_F + r_T \Delta_s - (1 - r_T - r_P)\Delta_e \tag{32}$$

where $r_T = \sigma_T/(\sigma_T + \sigma_B + \sigma_P) = \sigma_T/\sigma_F$ and $r_P = \sigma_P/(\sigma_T + \sigma_B + \sigma_P) = \sigma_P/\sigma_F$ are the mass flow-rate fractions of the top product stream and side-stream product, respectively. Equation (32) could be reduced to Eq. (24) as the same mass flow rate of both top and bottom product streams with the definition of $r = \sigma_P/\sigma_T = r_P/r_T$. By following the successive iteration method in the previous section of the same mass flow rate at both product streams, the repetitive calculations of Eqs. (29), (30), and (32) with the use of Eqs. (19)–(22) yield the values of Δ_s and Δ_e.

EFFECT OF OPERATING PARAMETERS ON DEVICE PERFORMANCE

There are many design and operating parameters that affect the device performance in the thermal diffusion column with sidestream operations. In such an event, the mass flow-rate ratio of the sidestream product (r), mass flow-rate fraction of top product stream (r_T), feed flow rate (σ_F), feed concentration (C_F), and feed position (ζ) may be the most significant factors. The variations of the degree of separation Δ with r, r_T, σ, C_F, and ζ are too complicated to express mathematically. However, their relationship was presented graphically as shown in Figs. 2–8. The degree of separation Δ decreases with increasing σ' (or mass flow rate of feed σ), as confirmed by Figs. 2 and 3 for the equal mass flow rate from both top and bottom products and mass flow-rate fraction variations of top product stream under sidestream

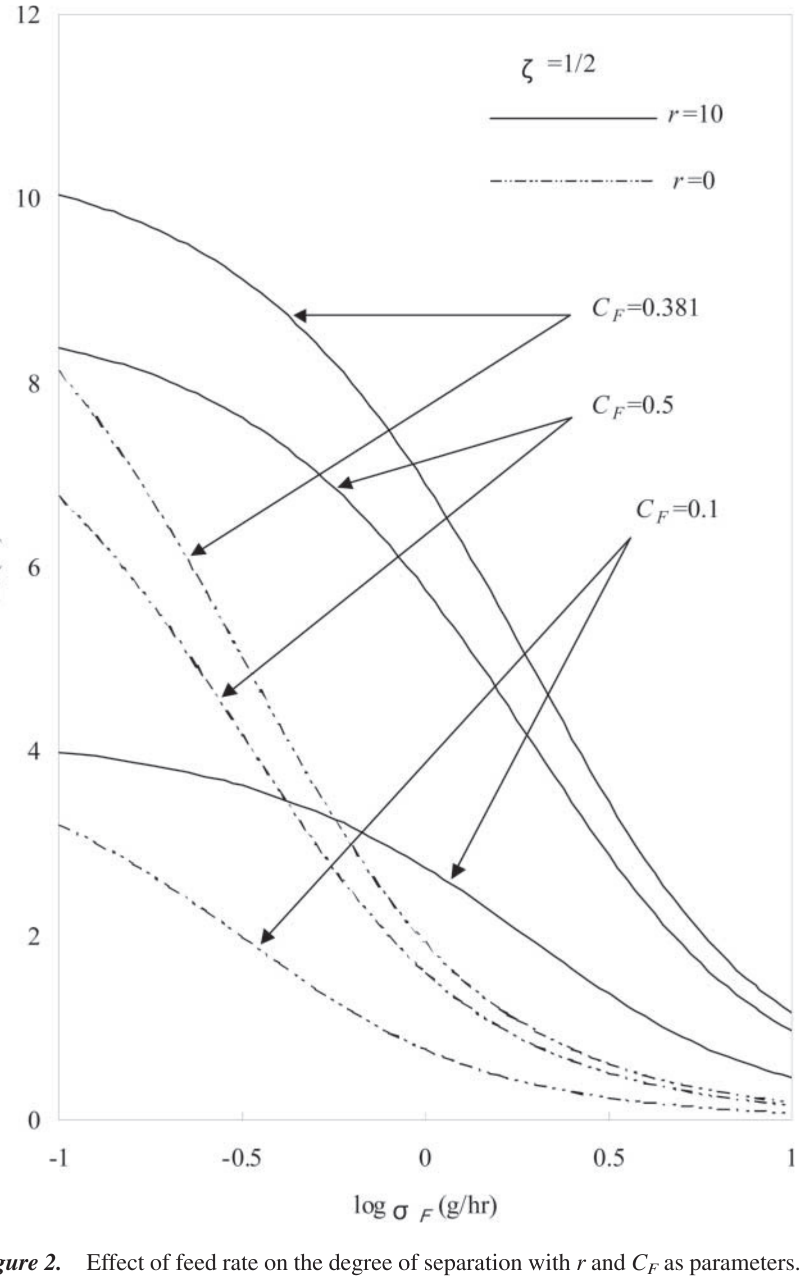

Figure 2. Effect of feed rate on the degree of separation with r and C_F as parameters.

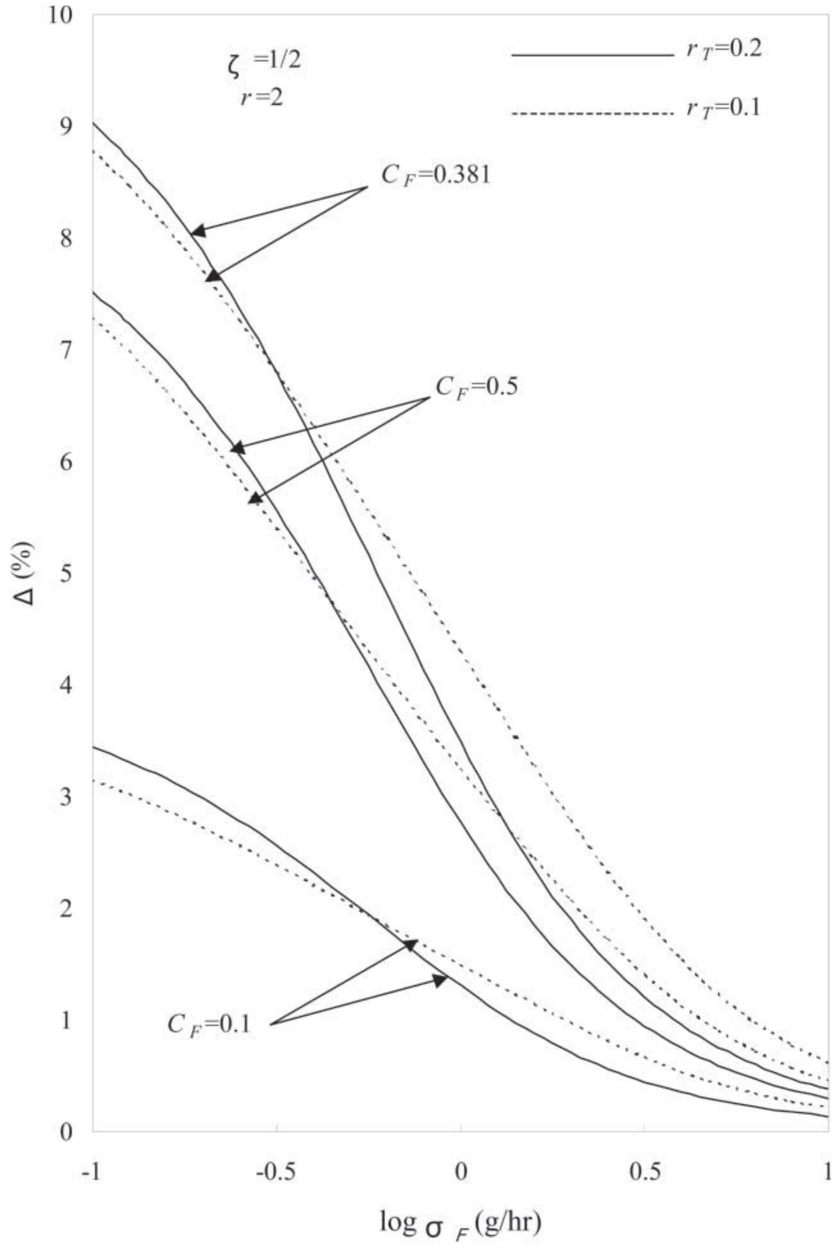

Figure 3. Effect of feed rate on the degree of separation with r_T and C_F as parameters.

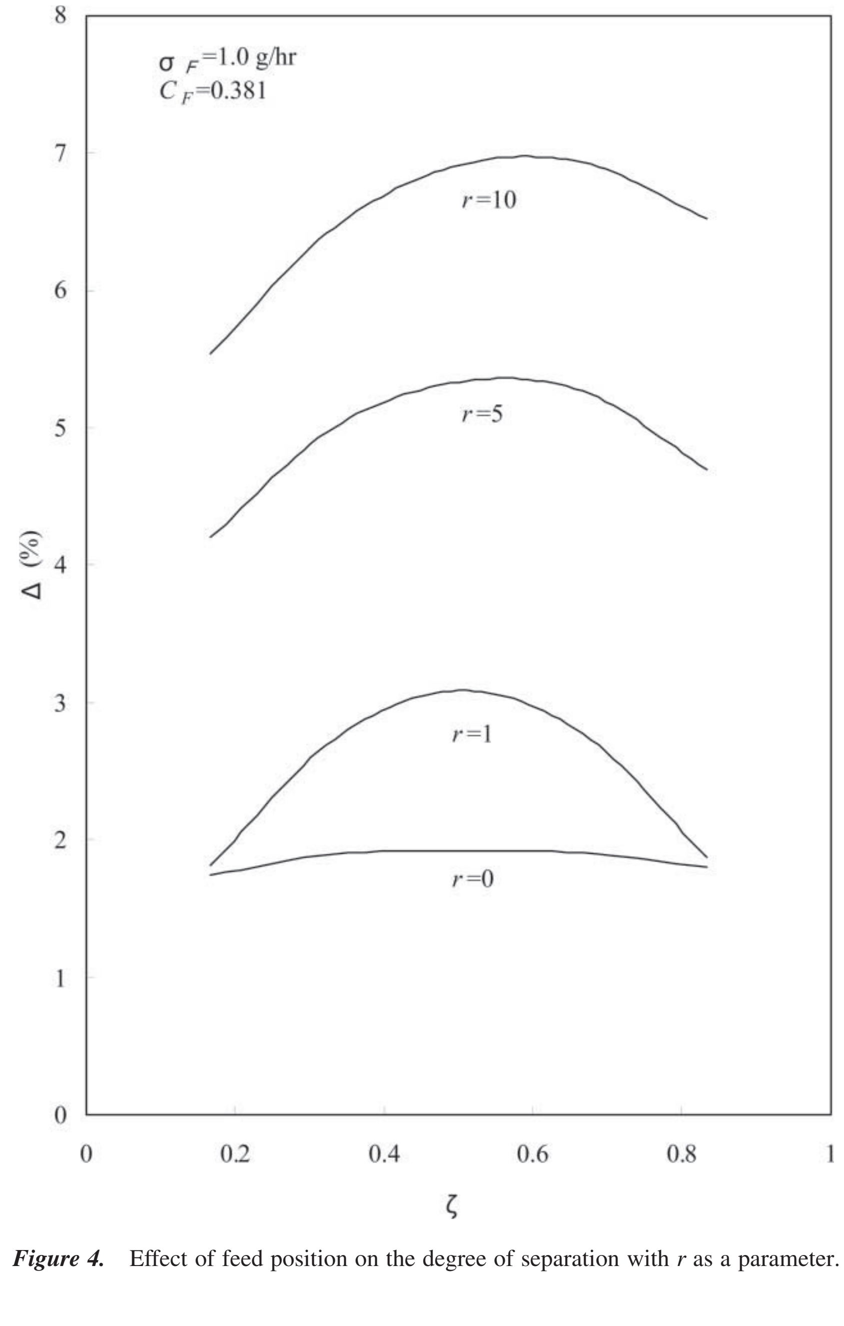

Figure 4. Effect of feed position on the degree of separation with *r* as a parameter.

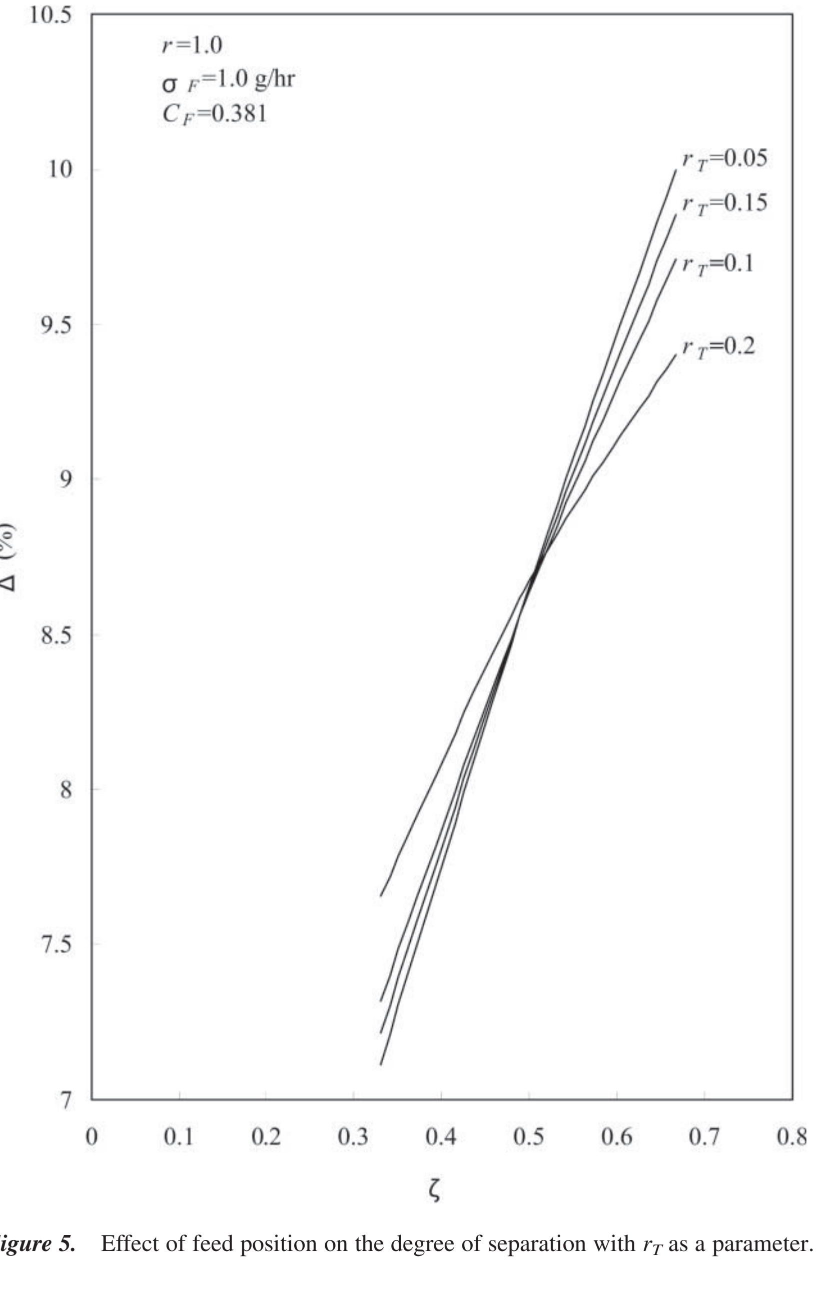

Figure 5. Effect of feed position on the degree of separation with r_T as a parameter.

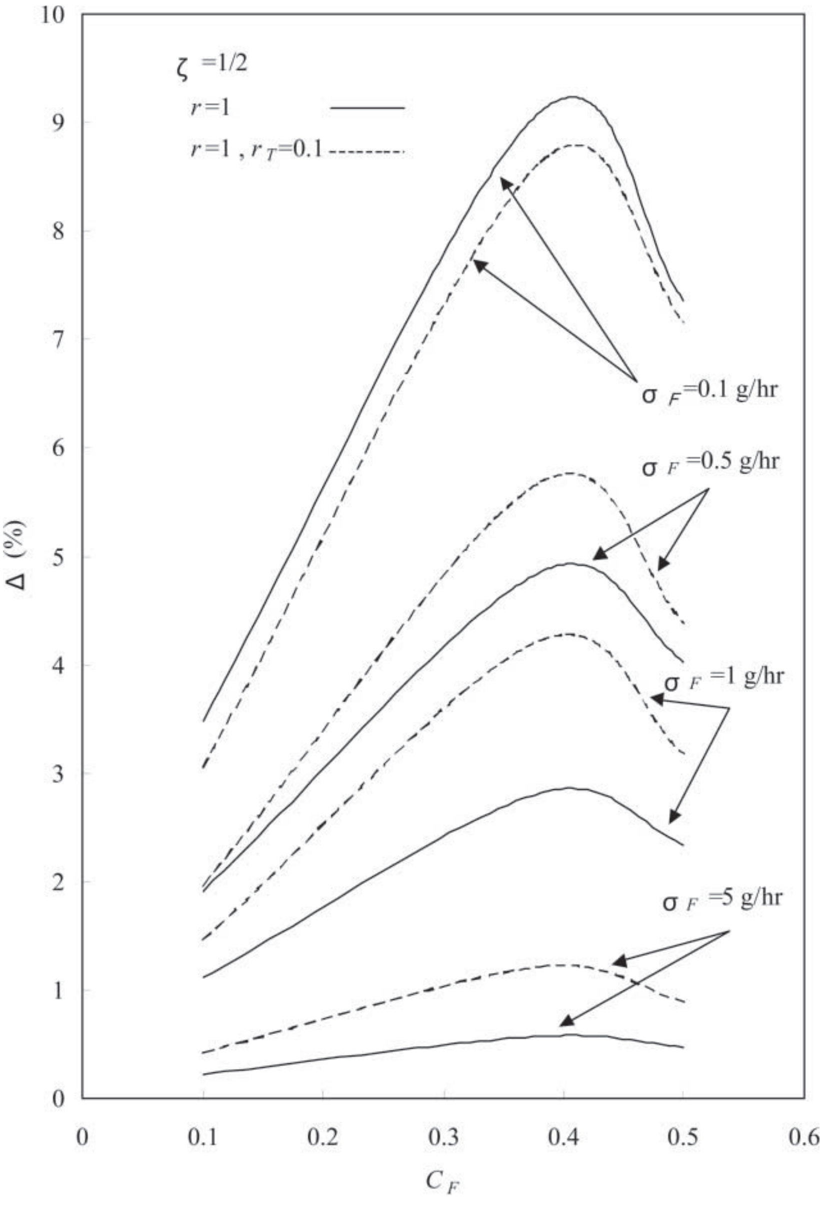

Figure 6. Effect of feed concentration on the degree of separation for the device under sidestream operations with feed concentration as a parameter.

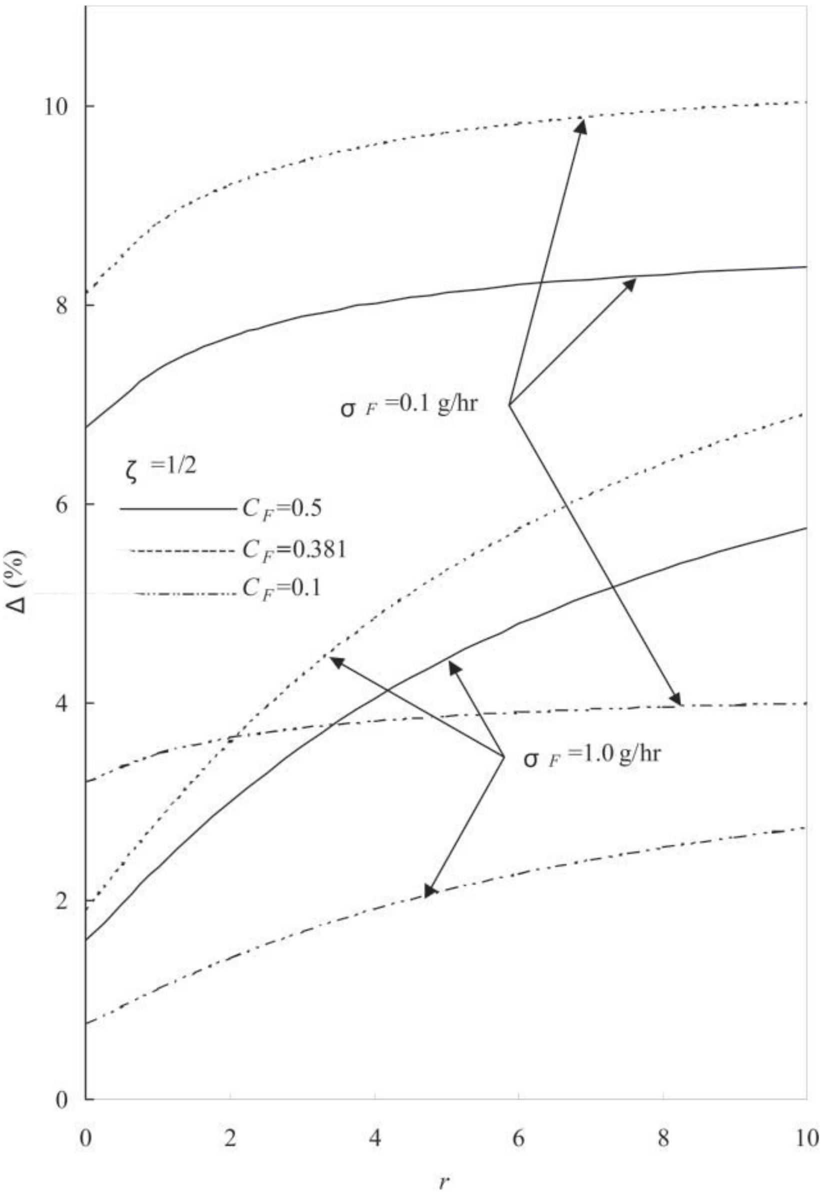

Figure 7. Effect of the mass flow-rate ratio of the sidestream product on the degree of separation with feed concentration and feed rate as parameters.

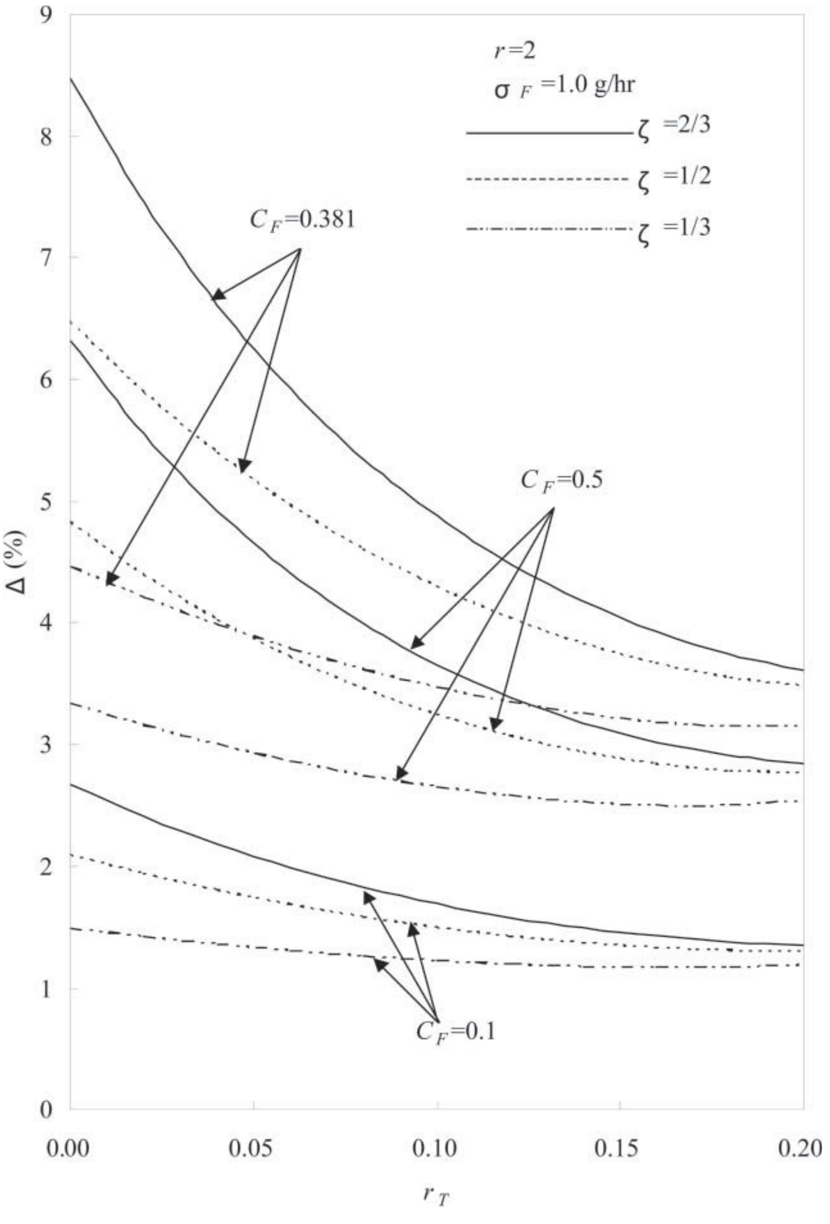

Figure 8. Effect of the mass flow-rate fraction of top product stream on the degree of separation with feed concentration and feed position as parameters.

operations, respectively. The tendency of the change of Δ with ζ and C_F is shown in Figs. 4 and 5 and Fig. 6, respectively. The tendency of the increment and decrement of Δ with r and r_T for the equal mass flow rate from both top and bottom product streams and mass flow-rate fraction variations of top product stream under sidestream operations, respectively, is shown in Figs. 7 and 8. The critical values of r and r_T during the calculation procedure should be selected in the allowable operation region for the device with sidestream operations, as shown in Fig. 9. Moreover, the feed position has much influence on the separation behavior, and the existence of ζ^* with flow-rate ratio variations of the sidestream product is also shown in Figs. 10 and 11.

EXPERIMENTAL STUDIES

A continuous-type concentric-tube thermal-diffusion column was constructed of stainless steel with the column length $L = 122\,\text{cm}$, circumference of length $2\pi R = 10\,\text{cm}$, and uniform annular space $2w = 0.04\,\text{cm}$, in which seven feed input and sidestream product points were drilled, to separate heavy water from water-isotope mixtures, as shown in Fig. 12. Hot and cold waters with specified temperature were supplied continuously from two tanks through the inner tube and jacket, respectively, to impose a temperature gradient on the mixture solution. The average surface temperatures of hot and cold surfaces were measured to be 47°C and 14°C in this experimental work, respectively, by four copper constantan thermocouples located on the surface ends of each plate. The mean temperature of the mixture solution ($(14 + 47)/2 = 30.5$°C) was used for the physical properties during the calculation procedure. The steady feed rate σ_F was regulated by a constant-head tank due to gravitational force into the selected inlet point of the thermal-diffusion column, and the flow-rate ratio variations of sidestream product were withdrawn at the opposite side. The top and bottom product streams as well as the sidestream product were attuned by needle valves and withdrawn continuously at $\zeta = 1/3$, $1/2$, and $2/3$ with the flow-rate fraction r_T, $(1 - r_T - r_P)$, and r_P, respectively, through cooling coils and rotameters to the collectors. An automatic density meter (model DA-210, Kyoto Electronics) was use to analyze at 25 ± 0.05°C the outlet sample products. The DA-210 density/specific gravity meter is of nature oscillation measurement type. Densities and specific gravities of liquid or gaseous substances can be measured to an accuracy of $\pm 1.0 \times 10^{-5}\,\text{g/cm}^3$. The specific gravity measurement was used to determine the isotopic concentration of heavy water, and the mass fraction of D_2O was calculated by appropriate equations.[23,24] The precision $\pm\, 5.0 \times 10^{-5}$ of D_2O mass fraction was achieved by this analyzer

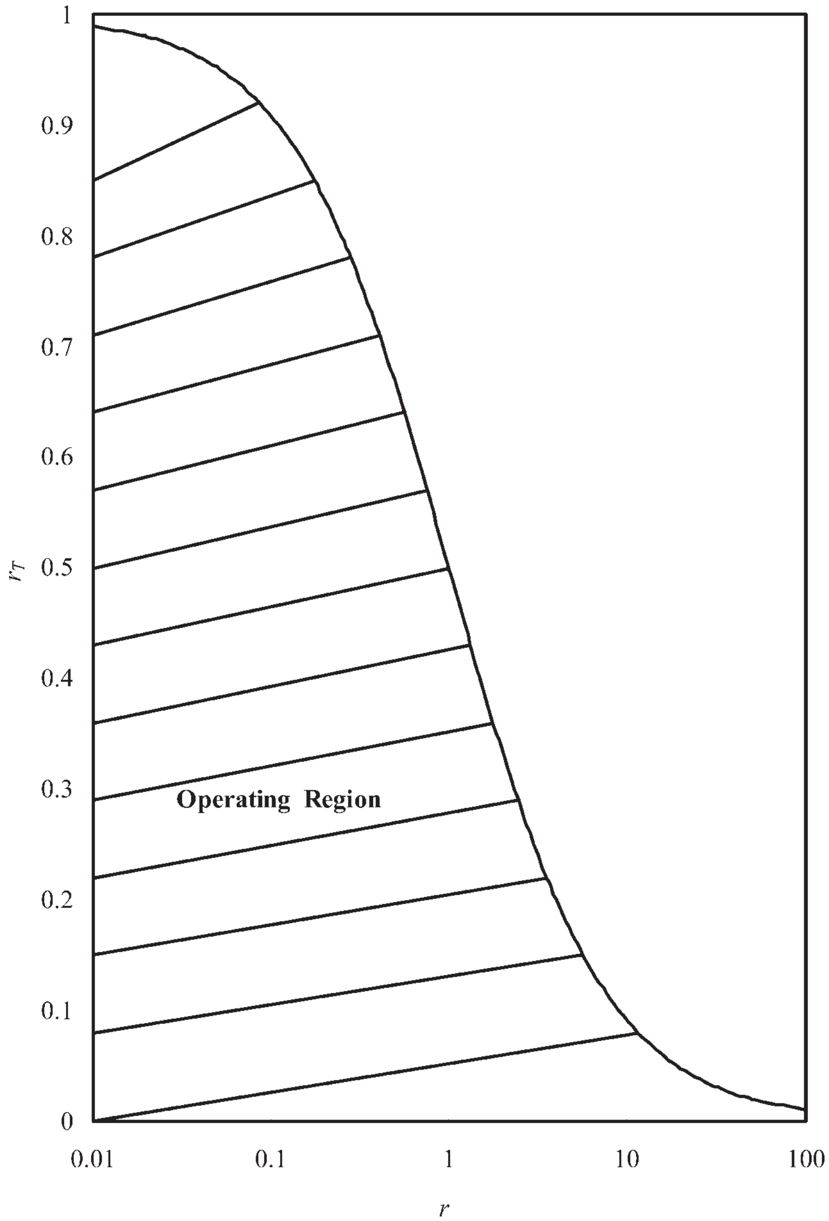

Figure 9. The critical values of r and r_T during the calculation procedure should be selected in the allowable operation region for the device with sidestream operations.

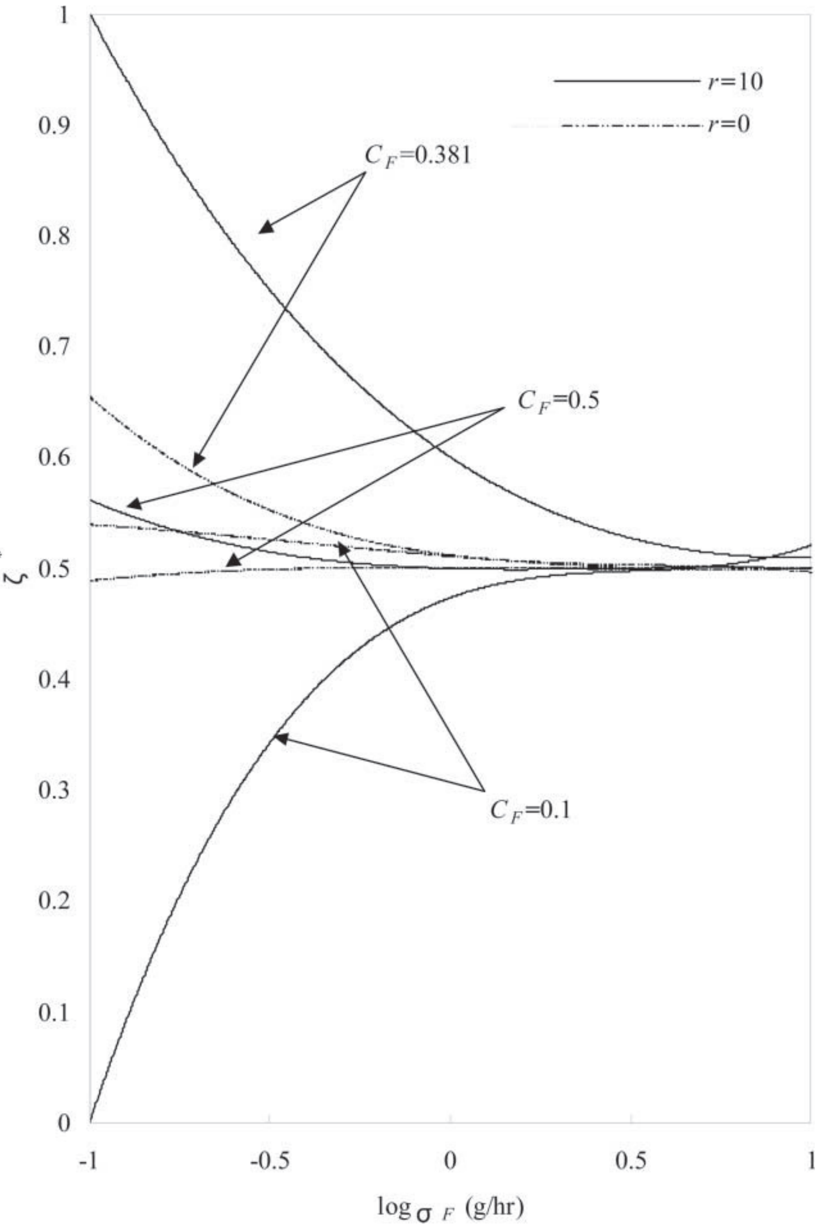

Figure 10. Best feed position for the maximum degree of separation with r and C_F as parameters.

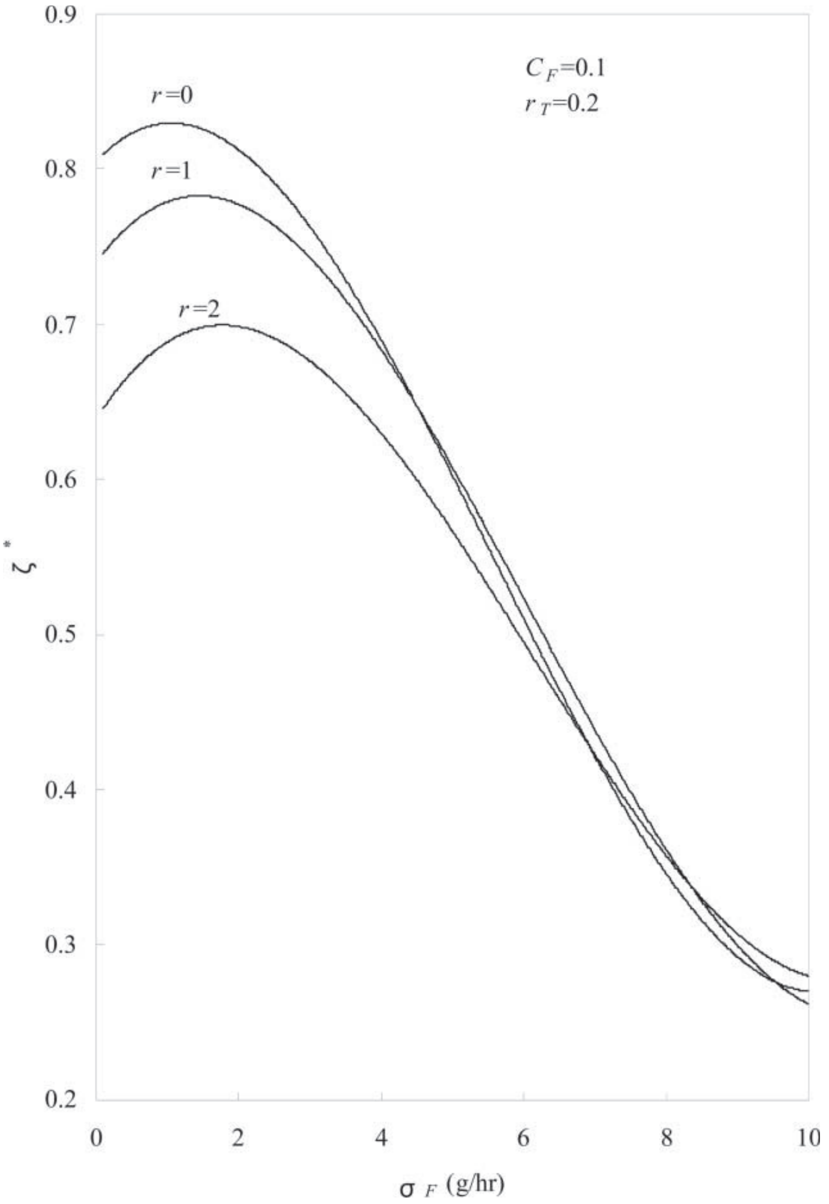

Figure 11. Best feed position for the maximum degree of separation with r_T and C_F as parameters.

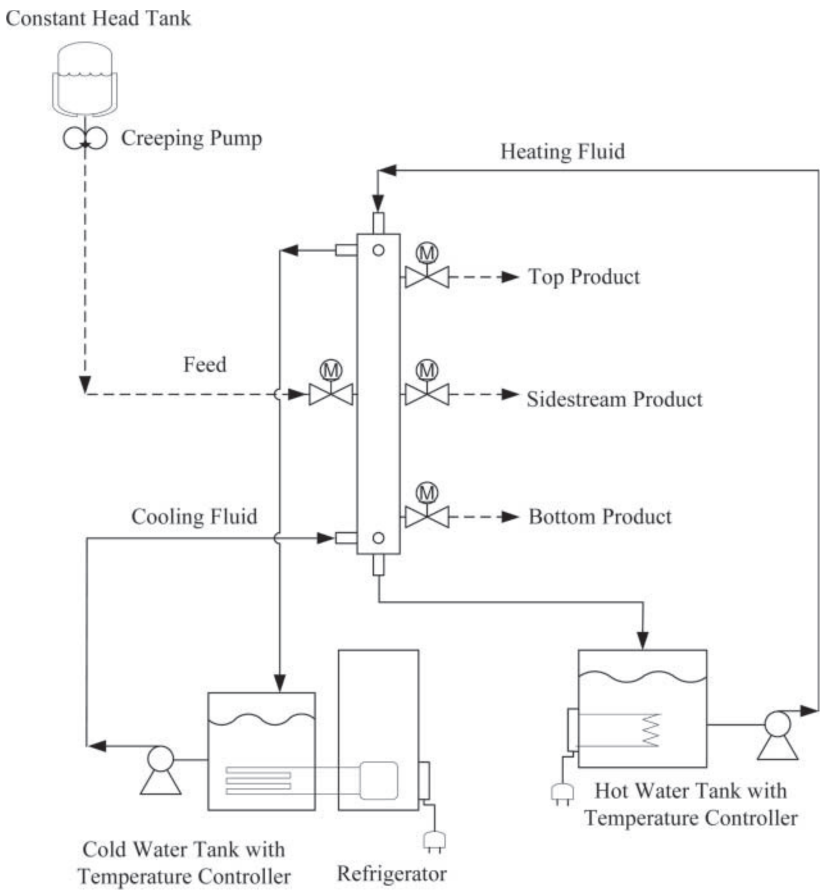

Figure 12. Flow diagram of the experimental system with sidestream operations.

in the present study. Comparisons of some results obtained in the experimental works with those calculated from theoretical solutions are represented in Figs. 13 and 14 under sidestream operations with $C_F = 0.381$ and $C_F = 0.1$.

SEPARATION EFFICIENCY IMPROVEMENT

The improvement of the modified thermal-diffusion column under sidestream operations with the mass flow-rate fraction variations of the top product stream and mass flow-rate ratio variations of the sidestream product

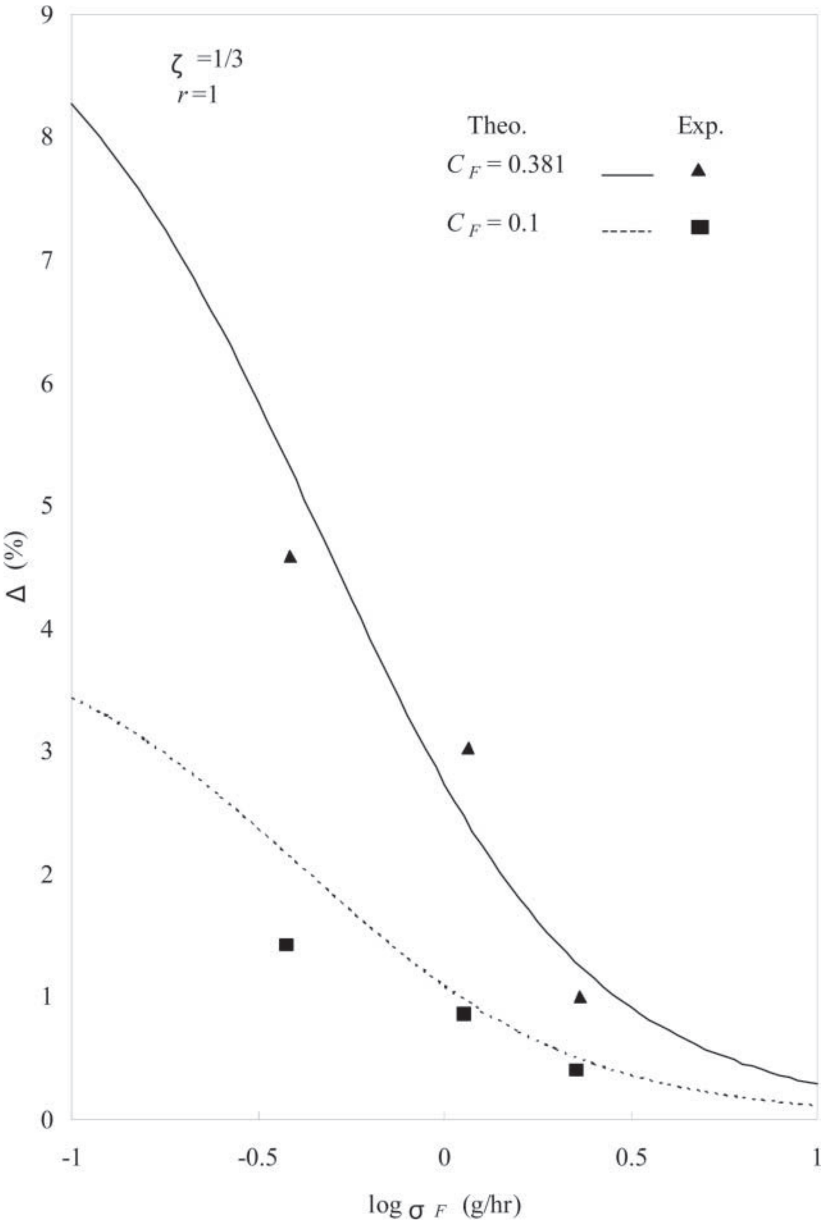

Figure 13. Comparisons of the degree of separation obtained from theoretical predictions and experimental works; $r = 1$.

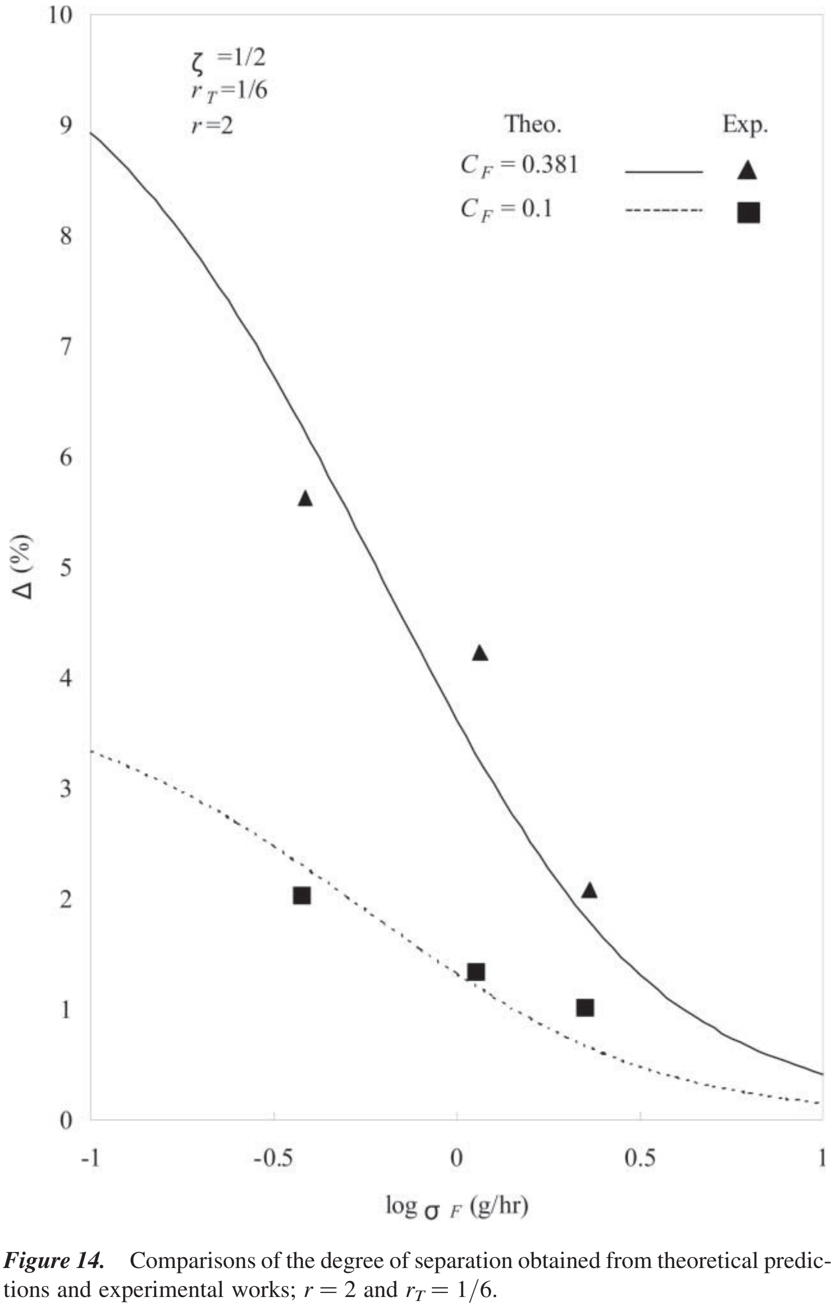

Figure 14. Comparisons of the degree of separation obtained from theoretical predictions and experimental works; $r = 2$ and $r_T = 1/6$.

is best illustrated by calculating the percentage increase in separation efficiency based on the classical Clusius-Dickel thermal-diffusion column as

$$I_r(\%) = \frac{\Delta_r(\text{with sidestream}) - \Delta_{r=0}(\text{Clusius-Dickel column})}{\Delta_{r=0}(\text{Clusius-Dickel column})} \times 100\% \tag{33}$$

$$I_{r,r_T}(\%) = \frac{\Delta_{r,r_T,\zeta}(\text{with sidestream}) - \Delta_{r=0,\zeta=0.5}(\text{Clusius-Dickel column})}{\Delta_{r=0,\zeta=0.5}(\text{Clusius-Dickel column})} \times 100\% \tag{34}$$

A numerical example with some equipment parameters and physical properties of the mixture for the heavy water enrichment is given as follows:[22]

$$H = -1.473 \times 10^{-4}\, g/s = -0.53\, g/hr$$
$$K = 1.549 \times 10^{-3}\, g \cdot cm/s = 5.5763\, g \cdot cm/hr$$
$$K_{eq} = 3.793$$
$$L = 122\, cm$$
$$B = 2\pi R = 10\, cm$$
$$2w = 0.04\, cm$$
$$\Delta T = 35\, K$$
$$\overline{T} = 303.5\, K$$
$$C_F = 0.1,\ 0.381,\ 0.5$$
$$\Delta T/2w = 875\, K/cm$$

A better comparison between the modified thermal-diffusion column under sidestream operations and classical Clusius-Dickel thermal-diffusion column has been made with products rates held constant. Thus, the column traffic and column usefulness would be the same. Some results are presented in Tables 1 and 2 for the continuous-type concentric-tube thermal-diffusion column with r and r_T as parameters under sidestream operations.

RESULTS AND DISCUSSIONS

The Degree of Separation in Devices with Sidestream Operations

Figures 2 and 3 show the degree of separation Δ vs. feed flow rate σ_F, respectively, for equal mass flow rates from both top and bottom products

Table 1. Comparison of the degree of separation obtained in the device under sidestream operations with that obtained in the classical thermal-diffusion column without sidestream operations; $\zeta = 1/2$.

	I_r (%)								
	$C_F = 0.1$			$C_F = 0.381$			$C_F = 0.5$		
σ_F (g/h)	$r = 1.0$	$r = 0.1$	$r = 0.01$	$r = 1.0$	$r = 0.1$	$r = 0.01$	$r = 1.0$	$r = 0.1$	$r = 0.01$
0.10	−6.61	2.49	4.11	13.46	24.41	26.37	−9.84	−1.14	0.42
0.13	1.58	12.34	14.30	22.52	39.33	42.19	−1.94	11.52	13.80
0.16	8.51	21.64	23.88	30.09	52.45	56.14	4.72	22.72	25.68
0.20	17.80	33.02	35.49	40.53	69.92	74.64	13.64	37.40	41.22
0.25	28.57	45.42	47.99	52.75	89.93	95.77	23.97	54.14	58.87
0.32	43.48	59.39	61.86	69.90	116.40	123.51	38.27	76.11	81.90
0.40	56.39	71.15	73.32	84.68	138.63	146.72	50.62	94.62	101.22
0.50	68.64	81.13	82.86	98.72	158.77	167.66	62.33	111.40	118.66
0.63	80.38	89.03	90.26	112.22	177.29	186.85	73.57	126.79	134.61
0.79	88.51	94.35	95.13	121.55	189.77	199.77	81.36	137.20	145.39
1.00	95.39	97.73	98.17	129.48	200.20	210.56	87.95	145.87	154.36
1.26	98.77	99.48	99.69	133.36	205.29	215.82	91.20	150.12	158.76
1.59	100.06	100.27	100.35	135.54	208.14	218.78	92.91	152.51	161.22
2.00	100.37	100.53	100.56	135.89	208.59	219.24	92.99	152.91	161.63
2.51	100.45	100.60	100.60	135.89	208.59	219.24	93.32	152.91	161.97
3.16	100.47	100.61	100.61	135.89	208.59	219.24	93.32	152.91	161.97
3.98	100.53	100.61	100.61	135.89	208.59	219.24	93.32	152.91	161.97
5.01	100.55	100.61	100.61	135.89	208.59	219.24	93.32	152.91	161.97
6.31	100.61	100.61	100.61	135.89	208.59	219.24	93.32	152.91	161.97
7.94	100.61	100.61	100.61	135.89	208.59	219.24	93.32	152.91	161.97
10.00	100.61	100.61	100.61	135.89	208.59	219.24	93.32	152.91	161.97

Table 2. Comparison of the degree of separation obtained in the device under the mass flow-rate ratio variations of the sidestream product and mass flow-rate fraction variations of the top product stream with that obtained in the classical thermal-diffusion column; $C_F = 0.5$, $r = 0.1$.

	I_{r,r_T} (%)								
	$\zeta = 1/3$			$\zeta = 1/2$			$\zeta = 2/3$		
σ_F (g/h)	$r_T = 0.1$	$r_T = 0.2$	$r_T = 0.3$	$r_T = 0.1$	$r_T = 0.2$	$r_T = 0.3$	$r_T = 0.1$	$r_T = 0.2$	$r_T = 0.3$
0.10	0.12	12.52	31.32	11.68	16.65	24.09	27.32	23.49	21.22
0.13	0.20	15.61	39.81	14.84	20.73	30.65	33.86	28.98	26.63
0.16	0.25	19.43	50.48	19.12	25.83	38.95	42.03	35.64	33.33
0.20	2.59	24.14	63.82	24.91	32.12	49.46	52.17	43.62	41.63
0.25	6.59	29.88	80.33	32.75	39.78	62.69	64.65	52.98	51.83
0.32	12.91	36.81	100.51	43.26	48.99	79.24	79.80	63.65	64.26
0.40	22.27	45.03	124.63	57.19	59.75	99.60	97.92	75.33	79.22
0.50	35.36	54.60	152.65	75.14	71.85	124.14	118.86	87.48	97.01
0.63	52.66	65.42	183.92	97.43	84.72	152.68	142.43	99.23	117.84
0.79	74.30	77.23	217.09	123.65	97.38	184.36	167.76	109.65	141.80
1.00	99.91	89.44	250.06	152.54	108.65	217.50	193.47	117.91	168.76
1.26	128.57	101.19	280.36	181.94	117.50	249.85	217.68	123.61	198.17
1.59	158.72	111.43	305.56	209.39	123.48	279.13	238.44	126.92	228.81
2.00	188.29	119.30	324.13	232.70	126.88	303.53	254.22	128.48	258.84
2.51	215.09	124.51	335.95	250.48	128.45	321.97	264.56	129.03	286.11
3.16	237.27	127.38	342.26	262.34	129.01	334.27	270.23	129.17	308.73
3.98	253.70	128.64	344.99	269.14	129.17	341.30	272.73	129.19	325.53
5.01	264.33	129.07	345.91	272.31	129.19	344.59	273.58	129.20	336.42
6.31	270.13	129.17	346.11	273.46	129.20	345.77	273.79	129.20	342.37
7.94	272.69	129.19	346.16	273.76	129.20	346.10	273.81	129.20	345.00
10.00	273.56	129.20	346.16	273.81	129.20	346.14	273.81	129.20	345.91

and mass flow-rate fraction variations of the top product stream under sidestream operations with the mass flow-rate ratio of the sidestream product (r) and mass flow-rate fraction of top product stream (r_T) as parameters while Figs. 4 and 5 show the degree of separation Δ vs. feed position ζ. It is seen for Figs. 2 and 4 that the larger the mass flow-rate ratio of the sidestream product r is, the better the degree of separation is, especially when the feed flow-rate σ_F decreases and the feed position is at $\zeta = 0.5$. Although the mass flow-rate fraction of top product stream r_T has positive influences on the degree of separation for the device under sidestream operations, the sidestream effect by increasing r_T and moving ζ toward the enriching section cannot compensate for the decrease of the pseudo concentration products, $C\hat{C}$. A graphical representation of the pseudo concentration products $C\hat{C}$ vs. C was plotted from our previous work[4] and the maximum value at $C_F = 0.44$. This is the reason why $C_F = 0.381$ performance is better than $C_F = 0.1$ and $C_F = 0.5$ performance, and hence the degree of separation decreases with increasing the mass flow-rate fraction of top product stream r_T for $\zeta > 0.5$ or as the feed concentration is greater than $\sigma > 0.32\,\mathrm{g/h}$ for $r = 2$. The effects of the feed concentration (C_F), mass flow-rate ratio of the sidestream product (r), and mass flow-rate fraction of top product stream (r_T) on the degree of separation are shown in Figs. 6–8, respectively. The variation of Δ with ζ is rather complicated and hard to show mathematically. However, there exists an optimal feed position ζ^* for obtaining the maximum degree of separation and the relation was presented graphically in Figs. 10 and 11 for operations with equal mass flow rates from both top and bottom products and mass flow-rate fraction variations of top product stream, respectively.

The experimental results of the degree of separation thus obtained with feed concentration and feed flow rate as parameters and the corresponding values of the theoretical predictions, calculated from Eqs. (14)–(16) for equal mass flow rates at top and bottom product streams, and from Eqs. (29) and (30) for the mass flow-rate fraction variations of top product stream, are plotted in Figs. 13 and 14 for comparisons. Performance of the experimental data is in good agreement with the theoretical predictions.

Improvement in the Degree of Separation with Sidestream Operations

Figures 2–8 and Tables 1 and 2 show that the degree of separation, Δ, and improvements of the degree of separation, I_r and I_{r,r_T}, respectively, of the device under sidestream operations with the mass flow-rate ratio of the sidestream product, mass flow-rate fraction of top product stream, feed flow rate, feed concentration and feed position (ζ) as parameters. The degree of separation efficiency of the device with sidestream operations is much larger than that of classical thermal-diffusion columns. The improvement of the degree of separation I_r increases with increasing the feed flow rate and mass flow-rate ratio of the sidestream product while the improvements of the degree of separation I_{r,r_T} increases as the mass flow-rate fraction of top product stream goes away from 0.2, especially for $r_T < 0.2$ with $r = 0.1$. But the increase with feed flow rate σ_F is high enough (say $\sigma_F > 2\,\mathrm{g/h}$).

CONCLUSION

The theoretical and experimental studies of the separation efficiency for the heavy water enrichment in a continuous concentric-tube thermal-diffusion column with sidestream operations have been investigated in the present study. The theoretical values of separation for various feed concentrations and feed rates were calculated from Eqs. (14)–(16) and Eqs. (29) and (30) for equal mass flow rates from both top and bottom products and variable mass flow-rate fractions of top product stream under sidestream operations, respectively, by using the given transport coefficients and equilibrium constant, and the effects of the mass flow-rate ratio of the sidestream product, mass flow-rate fraction of top product stream, feed flow rate, feed concentration, and feed position on the degree of separation are shown in Figs. 2–8, respectively. The mass flow-rate fraction of the top product stream and mass flow-rate ratio of sidestream product could suitably adjust the remixing effect and effectively scrub the undesired isotopes of water in the thermal-diffusion column, respectively, so the operating parameters r and r_T are introduced in this work. The separation efficiency in the new device is superior to that in the classical Clusius-Dickel thermal-diffusion column, as confirmed by Tables 1 and 2. Theoretical predictions, as shown in Fig. 2 as well as Tables 1 and 2, indicate that the advantage of the present device is evident. Moreover, the theoretical predictions confirm pretty well with experimental results, as illustrated in Figs. 13 and 14.

NOMENCLATURE

a_e, a_s	Constants defined by Eqs. (21) and (19), respectively (−)
$a_{e,0}$, $a_{s,0}$	Constants defined by Eqs. (21) and (19), respectively (−)
b_e, b_s	Constants defined by Eqs. (22) and (20), respectively (−)
$b_{e,0}$, $b_{s,0}$	Constants defined by Eqs. (22) and (20), respectively (−)
B	Circumference of length $2\pi R$ (cm)
C	Mass fraction concentration of heavy water in the H_2O-HDO-D_2O system (−)

C_B	C in the bottom product stream $(-)$
C_e	C in the enriching section $(-)$
C_F	C in the feed stream $(-)$
C_P	C in the sidestream product $(-)$
C_s	C in the stripping section $(-)$
C_T	C in the top product stream $(-)$
$C\hat{C}$	Pseudo product form of concentration for D_2O defined by Eq. (5) $(-)$
$C_e\hat{C}_e$	$C\hat{C}$ in the enriching section $(-)$
$C_s\hat{C}_s$	$C\hat{C}$ in the stripping section $(-)$
D	Ordinary diffusion coefficient (cm^2/s)
g	Gravitational acceleration (cm/s^2)
H	Transport coefficient defined by Eq. (3) (g/s)
I_r	Improvement of the degree of separation defined by Eq. (33) $(-)$
I_{r,r_T}	Improvement of the degree of separation defined by Eq. (34) $(-)$
J_{x-OD}	Mass flux of heavy water in the x-direction due to ordinary diffusion $(g/cm^2 \cdot s)$
J_{x-TD}	Mass flux of heavy water in the x-direction due to thermal diffusion $(g/cm^2 \cdot s)$
J_{z-OD}	Mass flux of heavy water in the z-direction due to ordinary diffusion $(g/cm^2 \cdot s)$
K	Transport coefficient defined by Eq. (4) $(g/s \cdot cm)$
K_{eq}	Mass-fraction equilibrium constant of the H_2O-HDO-D_2O system $(-)$
L	The column length, (cm)
L'	Dimensionless coordinate defined by Eqs. (13) $(-)$
L'_e	L' in the enriching section defined by Eqs. (13) $(-)$
L'_s	L' in the stripping section defined by Eqs. (13) $(-)$
r	Mass flow-rate ratio of the sidestream product $(-)$
r_T	Mass flow-rate fraction of top stream product $(-)$
R	Outside radius of inner tube in concentric tube columns, (cm)
R_e	The residual of square error in the enriching section defined by Eqs. (18) $(-)$
R_s	The residual of square error in the stripping section defined by Eqs. (17) $(-)$
T	Mean absolute temperature (K)
$\bar{T}$	Arithmetic mean value of T of hot wall and cold wall (K)
x	Coordinate in the horizontal direction (cm)
z	Coordinate in the vertical direction (cm)
z'	Dimensionless coordinate defined by Eq. (13) $(-)$

Greek Symbols

α	Thermal diffusion constant for D_2O in the H_2O-HDO-D_2O system, <0 (−)
$\bar{\beta}_T$	$(-\partial\rho/\partial T)$ evaluated at T (g/cm$^3\cdot$K)
Δ	Degree of separation, $C_B - C_T$ (−)
Δ_e	Degree of separation, $C_B - C_P$ (−)
Δ_s	Degree of separation, $C_P - C_T$ (−)
ΔT	Difference in temperature of hot and cold plates (K)
ζ	Feed position (−)
ζ^*	An optimal feed position (−)
μ	Absolute viscosity of fluid (g/cm·s)
$\bar{\rho}$	The mass density evaluated at $\bar{T}$ (g/cm^3)
σ	Mass flow rate of top or bottom product stream with equal mass rate (g/s)
σ'	The dimensionless mass flow rate defined by Eq. (13) (−)
σ_B	Mass flow rate of bottom product stream (g/s)
$\sigma_B{}'$	The dimensionless mass flow rate of the bottom product (−)
σ_F	Mass flow rate of feed (g/s)
σ_P	Mass flow rate of sidestream product (g/s)
σ_T	Mass flow rate of top product stream (g/s)
σ'_T	The dimensionless mass flow rate of the top product (−)
τ_e	Transport of heavy water along z-direction in enriching section (g/s)
τ_s	Transport of heavy water along z-direction in stripping section (g/s)
w	One-half of the plate spacing of columns (cm)

ACKNOWLEDGMENT

The authors wish to thank the National Science Council of the Republic of China for its financial support.

REFERENCES

1. Murphy, G.M. Ed.; *Production of Heavy Water*; National Nuclear Energy Series, III-4F, McGraw-Hill: New York, 1955.
2. Bebbing, W.P.; Thayer, V.R. Production of heavy water. Chem. Eng. Prog. **1959**, *55*, 70–78.

3. Yeh, H.M. Enrichment of heavy water by thermal diffusion. Chem. Eng. Comm. **1998**, *167*, 167–179.
4. Ho, C.D.; Yeh, H.M.; Guo, J.J. An analytical study on the enrichment of heavy water in the continuous thermal diffusion column with external refluxes. Sep. Sci. Technol. **2002**, *37*, 1–20.
5. Ho, C.D.; Chen, Y.T. The study of continuous thermal-diffusion columns on modified frazier-scheme for the enrichment of heavy water with column length varied at a constant ratio. Sep. Sci. Technol. **2003**, *38*, 2425–2445.
6. Clusius, K.; Dickel, G. Neues Verfahren zur Gasentmischung und Isotopentrennuug. Naturwissenschaften **1938**, *26*, 546–552.
7. Clusius, K.; Dickel, G. Grundlagen eines neuen Verfahrenz zur Gasentmischung und Isotopentrennung durch Thermodiffusion. Z. Phys. Chem. **1939**, *B44*, 397–450.
8. Furry, W.H.; Jones, R.C.; Onsager, L. On The theory of isotope separation by thermal diffusion. Phys. Rev. **1939**, *55*, 1083–1095.
9. Jones, R.C.; Furry, W.H. The separation of isotopes by thermal diffusion. Rev. Mod. Phys. **1946**, *18*, 151–224.
10. Power, J.E.; Wilke, C.R. Separation of liquid by thermal diffusion column. AIChE J. **1957**, *3*, 213–222.
11. Sullivan, L.J.; Ruppel, T.C.; Willingham, C.B. Rotary and packed thermal diffusion fractionating columns for liquids. Ind. Eng. Chem. **1955**, *47*, 208–212.
12. Ramser, J.H. Theory of thermal diffusion under linear fluid shear. Ind. Eng. Chem. **1957**, *49*, 155–158.
13. Sullivan, L.J.; Ruppel, T.C.; Willingham, C.B. Packed thermal diffusion column. Ind. Eng. Chem. **1957**, *49*, 110–113.
14. Yeh, H.M.; Ward, H.C. The improvement in separation of concentric tube thermal diffusion columns. Chem. Eng. Sci. **1971**, *26*, 937–947.
15. Pommer, L.; Fick, J.; Andersson, B.; Nilsson, C. Development of a NO_2 scrubber for accurate sampling of ambient levels of terpenes. Atmospheric Environment **2002**, *36*, 1443–1452.
16. Chien, T.W.; Chu, H. Removal of SO_2 and NO from flue gas by wet scrubbing using an aqueous $NaClO_2$ solution. J. Hazardous Materials **2000**, *B80*, 43–57.
17. Taylor, C.D.; Kovscek, P.D.; Thimons, E.D. Monitoring air flow through a machine-mounted dust scrubber. Appl. Occup. Environ. Hyg. **1996**, *11*, 813–816.
18. Ebert, F.; Buttner, H. Recent investigations with nozzle scrubbers. Power Technology **1996**, *86*, 31–36.
19. Lehner, M. Aerosol separation efficiency of a venturi scrubber working in self-priming mode. Aerosol Science and Technology **1998**, *28*, 389–402.

20. Mayinger, F.; Neumann, M. Dust collection in venture scrubbers. Ger. Chem. Eng. **1978**, *1*, 289–293.
21. Yeh, H.M.; Ho, C.D.; Yen, Y.L. Further study on the enrichment of heavy water in continuous-type thermal diffusion columns. Sep. Sci. Technol. **2002**, *37*, 1179–1198.
22. Standen, A. *Encyclopedia of Chemical Technology*, 3rd Ed.; Wiley: New York, 1978; Vol. 7, 549.
23. Kirshenbaum, I. *Physical Properties and Analysis of Heavy Water*; National Nuclear Energy Series III-4A, McGraw-Hill: New York, 1951; 247.
24. Yeh, H.M.; Yang, S.C. The enrichment of heavy water in a batch-type thermal diffusion columns. Chem. Eng. Sci. **1984**, *39*, 1277–1282.

Received January 2004
Accepted June 2004